Feasibility of UAV Based Optical Tracker for Tracking Australian Plague Locust

Nazifa Tahir*, Graham Brooker
Australian Centre for Field Robotics,
Rose Street Building J04, University of Sydney, NSW 2006
n.mariam@acfr.usyd.edu.au*, gbrooker@acfr.usyd.edu.au

Abstract

The paper discusses the development of an unmanned aerial vehicle (UAV) based optical system for tracking individual Australian plague locusts. Managing and monitoring of locust swarms is important for minimising damage to agriculture, and the optical tracker combines the benefits of aerial photography and tagged insects to help with this process. Optical transponders are attached to the upper thorax of individual locusts which are then tracked by a UAV mounted optical tracker. The paper analyses features of each component of the tracker and transponders, critical for the successful operation of the system and verifies them experimentally.

1. Introduction

Australia's encounter with pests such as the Australian plague locust is very old and has become important with the spread of agriculture. Monitoring and managing locust populations is essential for controlling crop damage as a result of population build up and swarm migration. Techniques like aerial photography, videography and remote sensing using lower frequency electromagnetic systems have been widely used for tracking and detecting of locusts in the past.

Aerial photography and videography provide real time monitoring [1] but lack high resolution and an insect identification capability. These techniques are only suitable for rapid survey and recording of large or inaccessible insect affected areas. Remote sensing techniques using vertical radar identify locust and grasshoppers by measuring wing beat frequencies [2],[3]. Vertical radar allows insects to be detected collectively over wide ranges which are not detectable by other techniques due to their small mass, low altitude flights and clutter offered by vegetations, crops etc. However, to obtain a detailed understanding of locust population dynamics and migration, monitoring of the behaviour of individual locusts in a swarm is important. At the present, such tracking is possible using harmonic radar, but it either allows tracking of individuals at short range [4] or is very expensive [5].

2. UAV based optical tracker

The paper presents a low cost unmanned aerial vehicle (UAV) based optical tracker for tracking Australian plague locusts employing a technique based on optics as illustrated in Figure 1. It combines the benefits of aerial photography and transponder tagging that allow for the surveying of large areas, as well as tracking individuals. In addition, the system is light and mobile when compared to harmonic radar.

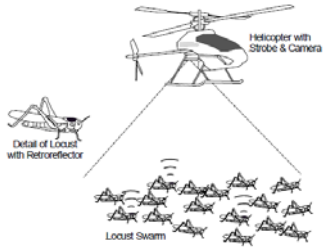

Figure 1: Illustration of working of UAV based optical tracker [6]

The following sections describe the selection criteria and requirements of each component critical for successful operation of the optical tracker.

3. Optical tracking system

The system consists primarily of the tracker mounted on a UAV and optical transponders fixed on locusts. It uses the UAV mounted strobe to illuminate the transponders and a camera for capturing the returns from them. The camera's exposure time and aperture are synchronized with the strobe to reject solar and other unwanted illumination.

The airborne portion of the system consists of the following major components: A PC/104 based computer, the strobe, a camera and the synchronizer as shown in Figure 2.

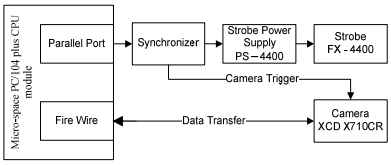

Figure 2: Block diagram of UAV mounted optical tracking system

3.1 Micro-space PC/104 plus CPU module [7]

The UAV payload developed at Australian Centre for Field Robotics (ACFR) consists of a Micro-space PC/104 plus with Intel ® Pentium ® CPU module along with a number of peripheral cards. Its main advantages are its low power consumption (12W to 25 W) and reliability which make it ideal to be use in an aircraft. In the prototype, the parallel port controls the synchronizer which in turn triggers the camera and strobe through adjustable delays. The CPU's Fire-wire interface is used to control the camera and to upload images which are then stored in compact flash memory for later analysis.

3.2 Strobe

The strobe is required to illuminate the transponders with sufficient energy to obtain good returns without affecting the behaviour of the locusts. The Perkin Elmer Strobe FX- 4400 was selected for this purpose. It generates a flash of about one Joule with an expected life of greater than 10^9 flashes [8]. Critical factors are the flash duration, its weight (and that of the associated electronics), and its field of view. The duration of the flash is 6μs [8], and it has been found that camera exposure times of about 13μs produce the best results given variations in the trigger delays through the flash electronics.

Obviously the mass of the strobe module should be as low as possible. The strobe head and its associated power supply (24 V PS-4400) weigh 125gm and 680gm respectively [8]. However, the weight of the power supply can be reduced by replacing the metallic casing by a plastic one, if appropriately shielded. The strobe illumination covers a field of view of 12° which plays an important role in determining the flying altitude of the UAV.

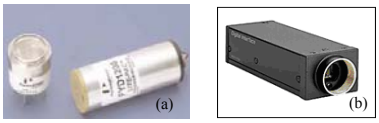

Figure 3 (a) Strobe FX-4400 (b) Sony fire-wire controlled digital camera XCD-X710 CR

3.3 Camera

The system requires a camera operating in the visible region of the light spectrum capable of interfacing with the PC/104. The Sony XCD-X710 CR camera, a member of the IEEE 1394 digital camera family, provides a high speed fire-wire interface (400 megabits/second). Its external trigger function allows it to capture fast moving and still images in a low light environment. This feature makes it ideal for the UAV based optical tracking system.

3.3.1 Frame rate

Mature locusts can cover 20km in a day [9]. However, the system is designed to track younger insects during their 4th or 5th instar, and these typically move about 1 m/min or about 500 m/day (depending on the temperature).

In relation to the speed of the fixed wing UAV (≈20m/s), the locust movement is insignificant. To cover a locust band, the UAV needs to cover a region of about 200×100m every minute, and that will advance by about 1 m every minute. The strobe rate depends on the size of the footprint on the ground, which is in turn dependent on the UAV height. At a height of 100m, the footprint is 21m in diameter, so assuming a 50% overlap, a new frame must be taken every 10m. This equates to an interval of 0.5s for a forward velocity of 20m/s.

The minimum time between consecutive frames is also limited by the time taken to charge the trigger capacitor of strobe power supply and the image storage time. The camera allows a frame rate of between 1.875 to 30 fps in format 0, mode 5 with colour coding Mono8 [10], so two frames per second is easy to achieve. The system has been designed to accommodate up to ten frames per second

3.3.2 Exposure time

The exposure time, τ (sec), defines the time during which the shutter of the camera remains open. The amount of energy gathered by the camera from sunlight is increases with an increase in exposure time, hence, to maximize the amount of light captured from the strobe, while minimizing the amount captured from solar illumination, the exposure time should be matched to the strobe duration and synchronized with it.. This requires that the shutter minimum exposure time should be $6\mu s \leq \tau < 15\mu s$. The XCD X710 CR camera allows a minimum exposure time of 10μs, however variable timing instabilities in the strobe trigger chain resulted in a 13.3μs exposure time being optimum.

3.3.3 Relative aperture

The aperture defines the light transmitting ability of a lens. The lens is usually fitted with an iris diaphragm which defines the diameter of the entrance pupil [4] in

units of relative aperture. This is also known as the f-stop or f-number and is given by

$$N = f/\# = \frac{f}{d}, \qquad (1)$$

where N or $f/\#$ is the f-stop, f (mm) is the focal length and d (mm) limiting aperture of the lens.

The amount of light passing through a lens is inversely proportional to the square of the f-stop, and the Sony XCD X710CR camera is fitted with a lens with focal length 6mm and f-stop 8.

3.3.4 Gain

The gain of the camera can be thought of as the process of electronically whitening the image. It is defined as the number of electrons required to increase output digital count by one. Mathematically it is given as [12]

$$\gamma = \frac{S}{D}, \qquad (2)$$

where γ is gain in electrons/digital count, S the signal level in electrons and D the digital count.

In a normal image, increasing the gain exposes the shadows providing more information about the dark regions. However, images taken by the optical tracker require no information about the background as they are binary in nature. The camera allows both manual and auto gain control from 0 to 18dB. In this application the gain is set to 0dB to ensure that the background remains black.

3.3.5 Field of view

Ideally the field of view of the camera should be matched to the strobe divergence. However, as the camera also provides information required to identify aircraft pose, a wider field of view is used. The field of view of Sony XCD- X710 camera is 50.8° × 41.5° corresponding to an image size of 1024×768 pixels.

3.3.6 Camera Noise

The performance of the camera is limited by sensor noise. This comes from quantum effects, variations and non uniformities in pixel size, material and often electrical interference. The Sony camera uses the Sony ICX 204AK charge coupled device (CCD) sensor. Its noise can be categorized as follows:

Shot noise: This is generated by the random arrival of photons onto a sensor pixel [13]. These electrons can be described by Poisson process which is dominant only at lower signal values.

Offset noise: Ideally, a zero should be read at all pixel locations in a completely dark frame (image made with the lens cap on and a short exposure time). However, due to the physics of the light-detection process, this value is not constant, and to maintain the distribution an offset is deliberately added to the output [14].

Dark current, I_{dark}: This is defined as the accumulation of electrons in each pixel due to thermal action [14]. It is the noise generated by the photo sensor current leakage independent of received photons [13]. It depends on the temperature, exposure time and some physical properties of the sensor and maintains a power law relationship with temperature [15].

Read noise or shading: With short exposure times and dark frames, the last pixel read off of the CCD has larger value than the first read off. This is because reading the pixels takes time and those waiting to be read accumulate charge from the dark current. This rate depends on temperature of the CCD and impurities in the pixel and is called as shading [14]. It is independent of exposure time. Similarly, the use of a long exposure time for capturing dim images also causes enough electrons to accumulate in each pixel to significantly affect the image. However, each pixel accumulates electrons at a different rate depending on its impurities. This may cause a faint pattern to form on images [14].

Also noticeable during longer exposure times is that some pixels are brighter than the surrounding background. These are called “hot pixels”. If a pixel always appears bright irrespective of the exposure, it is referred to as a “stuck pixel”. In our system, these problem pixels must be labeled and rejected as they could easily be identified as transponder returns.

Noise by on chip circuitry: Noise can be added to pixels from nearby on chip circuitry which may radiate infrared light. The accumulation of electrons due to this radiation is indistinguishable to accumulation of electrons due to dark current.

3.3.7 Eliminating the effects of noise

The magnitude of offset noise, shading and dark current values can be obtained by capturing a dark frame with an exposure time required for a typical dim image [14]. Such frames can be easily obtained by using neutral density filters.

In general, offset noise can be neglected as it is same for all pixels. While the effects of dark current, shading and read-out noise can be removed by dark frame subtraction. However, this requires dark frames taken at each different exposure time.

In each frame the pixel values correspond to the dark count (DC), which is defined as the product of the dark current with the exposure time [12]

$$DC = I_{dark}\tau_{shutter} \qquad \textbf{(3)}$$

Because the dark current is generated by random processes, it is convenient to obtain it as the slope of the mean dark count and exposure time of each dark frame.

3.4 Camera dynamic range

The dynamic range of a camera CCD is defined as its ability to detect very dim and bright parts of an image simultaneously. Mathematically, it is given as [16]

$$DR_{CCD} = 20\log\left(\frac{Full\ well\ capacity}{RMS\ Noise_{Dark}}\right) \qquad \textbf{(4)}$$

where *Full well capacity* is defined as the maximum possible signal (the saturation signal) and *RMS Noise*$_{Dark}$ is the root mean squared dark noise signal. For the Sony ICX 204AK CCD the saturation signal is 450mV and the RMS dark noise is 5.1mV [17]. This makes the theoretical, dynamic range of the CCD is 38.9 dB.

3.4.1 Experimental results

Experimentally the dynamic range of the CCD can determined using dark and flat frames while compensating for exposure, aperture and gain changes. A flat frame is obtained by taking a sequence of images of a white sheet at different exposure times. The slope of the plot of mean pixel or saturated count as a function of exposure time gives saturation signal.

For verification and validation of the results, flat frames were also taken with different exposure times using neutral density filters with optical densities, *OD*, of 0.3 and 0.6.

Optical density defines the darkness of a medium to light passing through it. The relationship between the *OD* and the transmittance, *T* is given by [11]

$$OD = \log_{10}\left(\frac{1}{T}\right) \qquad \textbf{(5)}$$

OD is related to changes in the f-stop of a camera lens which also governs the amount of light passing through an aperture. This relationship is defined as

$$1\ \text{OD unit} = 3.32\ \text{f stop} \qquad \textbf{(6)}$$

The experimental results are summarized in Figure 4. It shows the measured relationship between the exposure time and the pixel count for a clear aperture and for the two different neutral density filters covering the lens. The dark count is also plotted.

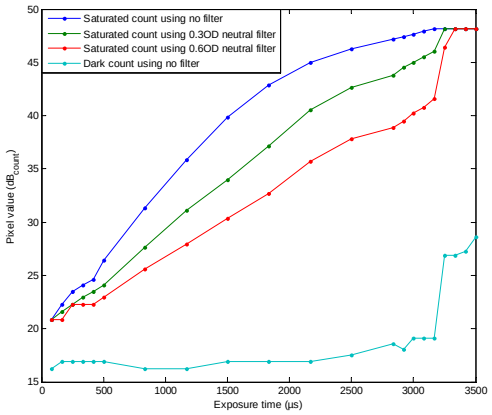

Figure 4: Plot of pixel value (dB$_{count}$) versus exposure time

In theory the saturated counts for the flat frame captured directly and through the two neutral density filters should be parallel and separated by 3dB when plotted on a log scale. However, it can be seen that this is clearly not the case with the traces converging for both short exposure times and at saturation for long exposure times. In addition, a doubling of the exposure time should result in a doubling of the saturated count (a change in 6dB) which also does not occur.

These issues notwithstanding, an estimate of the dynamic range of the camera can still be determined using the results in Figure 4. It reaches a maximum of about 31dB using the dark count level of 17dB for exposure times around 2ms and a camera saturation level of 48dB. The 8dB difference in the measured and theoretical result is due to the high dark count measured for the camera. To achieve the theoretical 38.9dB dynamic range requires that the dark count be about 2.9, and it is obviously much larger than that. It is possible that some of the difference may be due to the higher temperature of the CCD or to extraneous noise generated by the PC/104. However at the time of writing this discrepancy had not yet been resolved.

From the optical tracker perspective, this reduced dynamic range will have an adverse effect on the maximum range at which a transponder can be detected.

3.5 Synchronizer

The synchronizer electronics produces output pulses with the correct sense and duration for the camera and the strobe. In addition, monostable-based adjustable delays can be used to change the relative trigger times to allow for propagation delays through the strobe and camera trigger circuitry [18]. At present, the synchronizer is triggered by one of the lines of the parallel port of the PC/104 CPU module.

3.6 Optical transponder

The system requires a small optical transponder to be attached to the back of a locust. It should be capable of reflecting the incident light generated by the strobe back to a collocated camera. Retro reflecting prisms, trihedral corner reflectors and microsphere arrays exhibit this property and have been investigated [18].

The critical property required of these transponders is that they reflect all of the incident power back towards the source with minimum divergence. However, it was found that most commercial arrays are designed with some divergence to accommodate a wider viewing angle, and this decreased the light intensity to the camera to the extent that they were unusable.

A number of different diameter precision ground glass retro reflective prisms were used to verify the performance of the system. They were also used as a standard to which the lower cost plastic reflector clusters could be compared. A designer of plastic retro reflective arrays was contacted to determine whether similar performance to the glass reflectors could be achieved, but apparently this is not possible because diffraction effects, even in perfectly orthogonal trihedral arrays, result in significant divergence, and that produces a "star burst" pattern back at the camera.

A sheet of the best available retro reflective material was acquired for testing. It was scribed into sections comprising 3, 4, and 5 reflectors as shown in Figure 5, and the performance of these was compared to the glass devices.

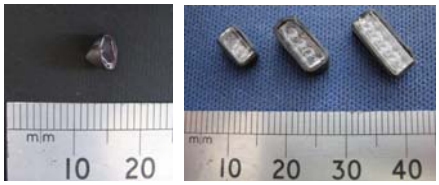

(a) **(b)**

Figure 5: A range of (a) glass and (b) plastic optical transponders, similar to those used in tests

3.6.1 Weight and size

Mature Australian Plague Locusts range in length from 20 to 45mm [19]. However, we are interested in tracking those during last instar at which stage they are about 16mm long, as shown in Figure 6. Because about one quarter of the length is available for the retro reflector, this limits the reflector length to be about 4mm. The width is limited to 2mm.

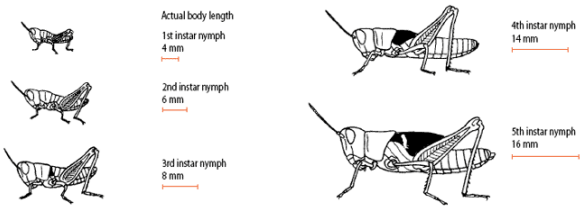

Figure 6: Plague locust showing position of retro reflector

The weight of the optical transponders is critical to the application and is limited by the locust's carrying capacity. Australian Plague Locusts are small (male last instar weighs 115± 3mg [20]), and though they are capable of carrying 1-2 times of their own mass, it is believed that this would modify their behaviour [21].

On consultation with the entomologists associated with this project, it was decided that, the weight of the transponder should be no more than 50% of weight of the locust, making it about 60 mg.

Whether the system will operate with such small transponders is a function of its aperture and the coefficient of luminance intensity. The latter is defined as the ratio of the reflected to incident light intensity. Because of their larger apertures, larger transponders can be detected over longer ranges. Therefore, the size of the reflector should be sufficient to ensure a high detection probability without altering the behaviour of the locust.

Table 1 compares the weight and dimensions of four transponders considered. It can be seen that even though Transponder D has suitable dimensions it is still really too heavy to be carried by the locust.

Table 1: Comparison between different optical transponder

	Prisms	Material	Aperture (mm^2)	Depth (mm)	Weight (mg)
A	1	Glass	38.48	6	360
B	5	Plastic	23.67	3.03	180
C	4	Plastic	18.94	3.03	150
D	3	Plastic	14.20	3.03	140

3.6.2 Beam divergence

One of the critical factors that limits the performance of retro reflectors for use as optical transponders is the beam divergence. Some beam divergence is essential as it ensures that a portion of the transponder return enters a camera mounted adjacent to the strobe. As the beam divergence decreases below this critical angle, proportionally less will enter the camera and the detection probability will be reduced. More complicated optics using a beam splitter and a couple of prisms could be used to combine the apertures of the strobe and the camera but this would add significantly to the cost of the sensor.

All retro reflectors are divergent to some extent as determined by the diffraction limits of the aperture. Calculations show that for the perfectly manufactured glass reflectors this will vary between 300μrad for a 2mm reflector to 100μrad for a 5mm reflector. Laser based measurements made using the plastic reflectors show much worse results with measured divergences of approximately 9.5 mrad and 7.9 mrad for reflectors with 4 and 3 prisms respectively, as shown in Figure 7.

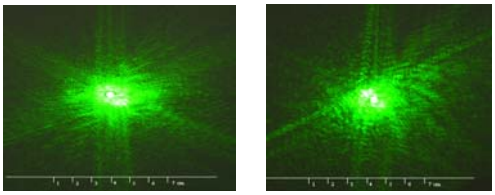

(a) (b)

Figure 7: Measured beam divergences of transponders at 3.68 m for (a) transponder C (4 prisms) (b) transponder D (3 prisms)

3.6.3 Relative illuminance

An attempt has been made to characterise the performance of the optical transponders by capturing images of the individual strobe illuminated reflectors.

Figure 8 compares the relative illuminance the four transponders. It can be seen that the glass reflector performs best and that the plastic transponder, D, made up of the fewest prisms performs worst. At a range of 50 to 55m its illuminance has been reduced to 50% of the saturation level. The other transponders, made up from more prisms, perform marginally better, but their improved performance is not commensurate with their increased mass. The significantly poorer performance and wider divergence of the plastic transponders, when compared to their glass counterpart, is not well understood and is subject to further investigation.

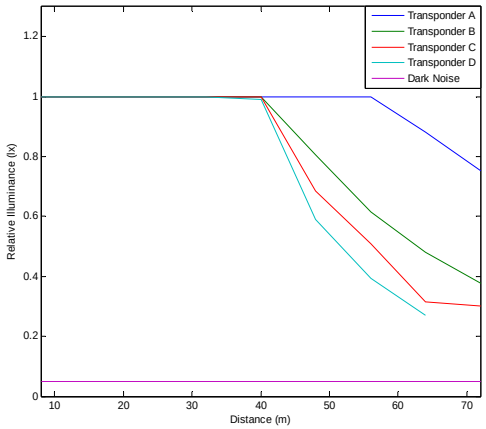

Figure 8: Comparison of relative illuminnace of different transponders at different distances

3.6.4 Camera gain setting

In theory, the gain of the camera should have minimal effect on the performance of the system. However, as shown in Figure 9, there is an increase in the level of background illumination which would reduce the effective signal to noise ratio of the transponder somewhat. In addition, the level of the dark noise would increase with the result that the camera dynamic range would also be reduced. For these reasons, a gain of 0dB has been selected as appropriate.

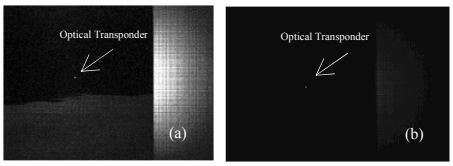

Figure 9: Images taken in sunlight by the optical tracker with exposure time 10μs and (a) high camera gain (b) low camera gain

3.6.5 Camera exposure time settings

As explained in section 3.3.2, an exposure time of $\tau_{shutter}$ = 13.3μs synchronises the strobe and the camera. Figure 10 shows that the relative illuminance of the transponder is higher, at a given range when exposure time is set to 13.3μs compared to that at 10μs. This discrepancy has been attributed to a slight and unpredictable delay in the strobe trigger relative to that of the camera. Unfortunately this increase in exposure time also increases the amount of sunlight striking the CCD, making the background visible, as evident in Figure 11. However, the relative contrast is still sufficient to detect the transponder.

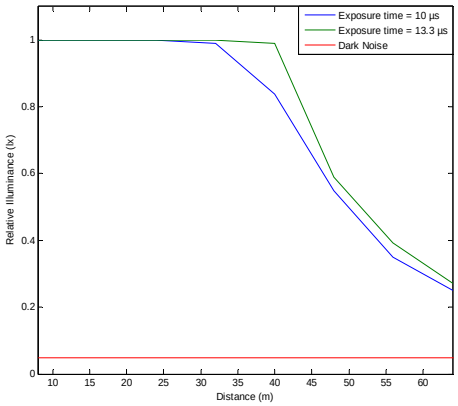

Figure 10: Relative illuminance of transponder D with different camera exposure time settings

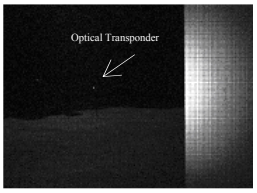

Figure 11: Image taken in sunlight by tracker with low camera gain and exposure time 13.3 µs

3.7 Optical tracker requirements

For successful operation of the UAV-based optical tracker, issues related to minimum height, line of sight and signal to noise ratio must also be addressed.

3.7.1 Optical tracker coverage area

The overall coverage area of the optical tracker is limited by the field of view of the strobe which is only 12° [8] and is significantly smaller than the field of view of the camera. Figure 12 compares the coverage area of the strobe and camera at different heights above ground. The coverage of the strobe can be made equal to that of camera by using a divergent lens, but this comes at the expense of a decrease in intensity of the returns from the transponder.

The height above ground is also limited by the transponder performance as described in section 3.5.3, and also the size of a camera pixel. The instantaneous field of view of a pixel defines the resolution of the system and therefore determines the minimum distance between two locusts that will allow them to be identified as individuals. Ideally, this resolution will be as good as possible, but it is limited by the number of pixels in the CCD array and the field of view of the camera. For this project a resolution of 0.25m is adequate. The pixels of the XCD X710CR camera fitted with a lens of focal length 6mm are square with an instantaneous angle of view of α = 0.05deg (870µrad) [19]. The area of a pixel on the ground, A_{pix} (m^2), is given by

$$A_{pix} = H^2\alpha^2 \qquad \textbf{(7)}$$

where α (rad) is the instantaneous angle of view of a single camera pixel.

This equates to a cross-range footprint that increases linearly with height and an area that increases with the square of the height. For the required resolution, UAV heights up to more than 300m can be accommodated.

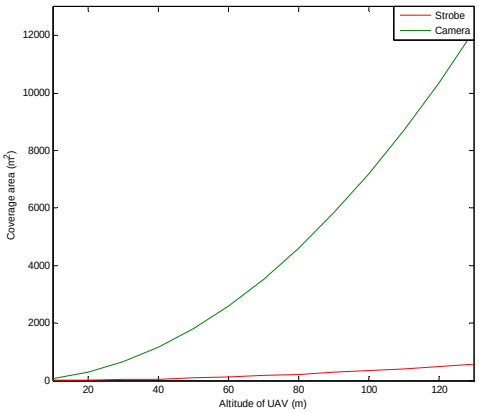

Figure 12: Comparison of coverage area of strobe and camera at different flying altitudes.

3.7.2 Line of sight requirement

Due to the properties of the lens system projecting onto a flat CCD array, the centre pixels of an image are brighter than those off towards the edges. The light intensity projected onto the array as a function of the distance from the centre point is given by the relationship [14]

$$I = \frac{1}{D^2} \qquad \textbf{(8)}$$

where I is the relative intensity of a ray of light and D is its distance from centre point.

It is difficult to completely remove this effect. However, this effect is small and the transponders away from the direct line of sight should still be detected if the returns are higher than the system noise.

3.7.3 Signal level back at the camera

It is not practical to use the same aperture for the strobe and the camera, therefore they are mounted adjacent one another. This requires that the transponders have sufficient divergence to ensure that the reflected power illuminates the camera aperture.

The total power radiated by the strobe can be calculated from the energy discharged from the HV capacitor bank, the efficiency of the conversion to light and the duration of the flash

$$P_S = \frac{E_S \eta}{T_S} \qquad \textbf{(9)}$$

where P_s (W) is the total power radiated by strobe, E_s (J) strobe energy, η efficiency and T_s is the duration of the flash. For FX-4400 T_s = 6μs and E_s = 1 J. Assuming an efficiency of 100%, this equates to a radiated power P_s = 166.7 kW.

The power density of the strobe light on the ground is

$$S_i = \frac{P_s}{A_s} \qquad \textbf{(10)}$$

where S_i (W/m^2) is the power density and A_s (m^2) is the area illuminated by the strobe.

For a strobe divergence angle, θ_s (rad), the area illuminated by the strobe, as a function of height, can be written as

$$A_s = \frac{\pi(H\theta_s)^2}{4} \qquad \textbf{(11)}$$

Combining (10) and (11) to determine the power density on the ground

$$S_i = \frac{4P_s}{\pi H^2 \theta_s^2} \qquad \textbf{(12)}$$

The transponder with aperture A_t (m^2), intercepts a small fraction of the power and reflects it back toward the camera. The total power reflected back towards the camera is equal to the product of the strobe power density on the ground and the aperture of the transponder

$$P_{ref} = S_i A_t = \frac{4P_s A_t}{\pi H^2 \theta_s^2} \qquad \textbf{(13)}$$

Assuming that the divergence of the reflected beam is ϕ_t (rad), then the power density at the camera is

$$S_{rc} = \frac{P_{ref}}{A_{rec}} = \frac{4P_{ref}}{\pi H^2 \phi_t^2} \qquad \textbf{(14)}$$

Combining (13) and (14) to simplify the equation describing the power density back at the camera

$$S_{rc} = \frac{16P_s A_t}{\pi^2 H^4 \theta_s^2 \phi_t^2} \qquad \textbf{(15)}$$

It is important to remember that the transponder divergence, ϕ_t, must be sufficiently wide to illuminate the camera at the operational height of the system.

The amount of solar power, P_{sun} (W), competing with that from the transponder is a function of the solar power density on the ground, S_{sun} (W), and the area of a pixel on the ground, A_{pix} (m^2) as determined from the instantaneous field of view of the camera and the height.

$$P_{sun} = A_{pix} S_{sun} = H^2 \alpha^2 S_{sun} \qquad \textbf{(16)}$$

For a ground reflectivity, ρ, and for uniform scattering over the forward hemisphere, the solar noise power density for each pixel back at the camera is

$$S_{sc} = \frac{P_{sun}\rho}{2\pi H^2} \qquad \textbf{(17)}$$

Substituting (16) into (17) and simplifying

$$S_{sc} = \frac{S_{sun}\alpha^2 \rho}{2\pi} \qquad \textbf{(18)}$$

This is a satisfying result as it confirms that the brightness of a camera pixel is independent of the distance to the ground.

3.7.4 Signal to noise ratio

To determine the signal to noise ratio of the system, the transponder energy density back at the camera is compared to that of undesired signals caused by reflections from the ground from both the strobe and the sun. The reason that the power density cannot be used is that the durations of the signals may be different, and the camera provides an output that is determined by the exposure time.

Obviously if a large natural retro, or aligned specular reflector, such as a pool of water, is present in the same pixel as the transponder, then the return from the locust will be swamped. However, in general, the ground can be considered to scatter isotropically, and with a fairly low reflectivity (depending on the terrain type).

$$SNR_{dB} = 10\log_{10}\frac{S_{rc}\tau_{strobe}}{S_{sc}\tau_{shutter}} \qquad \textbf{(19)}$$

where τ_{strobe} (sec) is the duration of the strobe pulse and $\tau_{shutter}$ (sec), is the exposure time. Considering the following values, which are typical for the system:

Strobe power: P_s = 166.7kW
Transponder aperture: $A_t = 14.205\times10^{-6}$ m^2
Strobe divergence: θ_s = 0.21rad (12°)
Transponder divergence: ϕ_t = 7.9 mrad
Solar albedo: S_{sun} = 500 W/m^2
Camera pixel angle of view: α = 0.87mrad
Ground reflectivity: ρ = 0.2
Strobe duration: τ_{strobe} = 6μs
Exposure time: $\tau_{shutter}$ = 13.3μs

The signal to noise ratio as a function of height is shown in Figure 13.

If the spacing between the centre of the strobe and the centre of the camera lens is 50mm and the lens

diameter is 25mm, then the camera aperture will be fully illuminated at heights greater than 20m

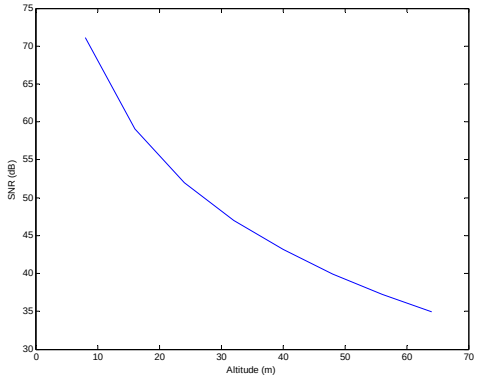

Figure 13: Strobe signal to solar noise ratio in a single camera pixel as a function of height

3.7.5 Relating measurement to theory

The received signal level from a flat frame shown in Figure 4 is 41dB$_{count}$ for an exposure time of 1.5ms. If a linear relationship between exposure time and saturated count is assumed, this equates to 0dB$_{count}$ for an exposure time of 13.3µs. A camera saturation level of 48dB$_{count}$ would therefore occur at a SNR of 48dB. From Figure 15 this occurs at a range of about 40m compared to a solar illuminated white background.

If Figure 13 is redrawn in linear space, normalized to a saturation level of unity, occurring at a range of 40m, then the theoretical performance of a 3×3mm transponder can be determined. Figure 14 shows a comparison between this theoretical result and the measured results for a similar sized transponder (taken from Figure 8).

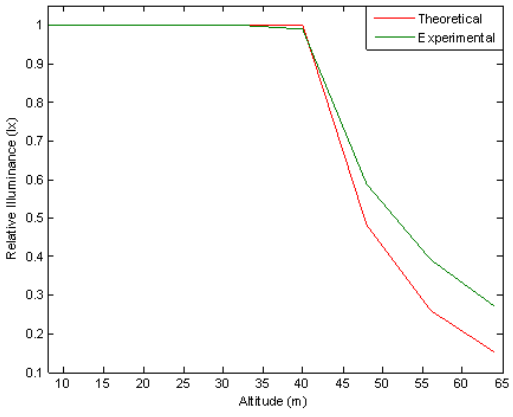

Figure 14: Theoretical and measured relative illuminances of a transponder D (3 prisms) seen by the camera

It can be seen that there is good agreement between the theoretical and the measured results.

3.8 System software

The strobe and camera are controlled through Linux operating system based software running on Micro-space PC/104 plus CPU module of the UAV. Linux guarantees highly reliable performance in a real-time environment. The software is developed in C language and uses libdc1394.lib and libraw1394 libraries.

A flowchart showing the application is shown in Figure 15.

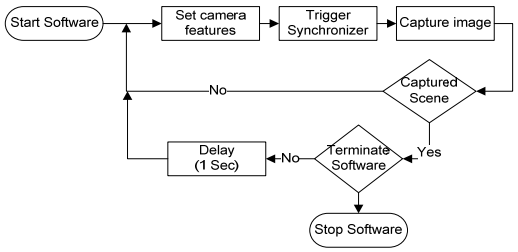

Figure 15: Flow chart of optical tracker software

In its current form, the software takes a pair of images sequentially (with minimum possible delay). The first image is configured to with an exposure time of 13.3µs, and occurs simultaneously with the firing of the strobe. The second is configured for an exposure time of about 167 µs to capture a gray scale image of the scene. The process is repeated once every second, or possibly more often so that a mosaic of the visible images can be constructed to identify the position and attitude of the aircraft relative to the ground.

Because of the short interval between the images in each pair, the strobe images showing only the positions of the tagged locusts can easily be superimposed onto the visible image mosaic to determine the positions of the locusts. As the flight progresses a larger and larger mosaic can be constructed with the paths of individual locusts indicated by their bright returns as shown in the following simulation.

4. Experimental results

Initial experiments have been carried out on the ground with the transponder attached to a tripod against a well illuminated background as shown in Figure 16a. Figures 16 (b), (c) and (d) show the detection of Transponder D, C and B respectively at a distance of 40m from the system. For convenience of visibility the colours of images have been inverted.

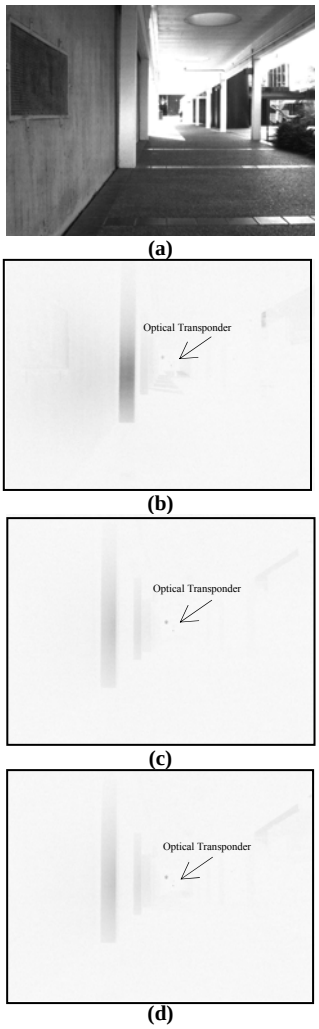

Figure 16: (a) Ground test area (b) Return from transponder D (c) transponder C (d) transponder B at a distance of 40m from the system

5. Conclusions and future work

The paper presents the feasibility of UAV based optical system for tracking the Australian Plague Locusts. It describes in detail the selection criteria and requirements of each component of the system. Initial experiments conducted on ground show that the performance of optical tracker can easily identify locusts from a height of 50m, and depending on the sophistication of the image thresholding software, from higher than this. However, until the shortcomings of the low-cost transponders can be addressed, the overall system performance will be limited, or users will have to be prepared to sacrifice expensive, but high performance glass retro reflectors during field trials.

Acknowledgements

The authors would like to acknowledge Alex Wendel as the developer of the original prototype, Paul Thompson for his help in configuring the computer hardware and, of course, Greg Sword and his biologists for their encyclopedic knowledge of the characteristics and behaviour of the Australian Plague Locust.

References

[1] Riley, JR "Remote sensing in entomology". Ann. Rev. Ento. 1989

[2] Schaefer, GW "Radar studies of locust, moth and butterfly migration in the Sahara". Proc. Roy. Ent. Soc. Lond. C 1969

[3] Riley, JR, Reynolds, DR "Radar-based studies of the migratory flight of grasshoppers in the middle Niger area of Mali. Proc. R. Soc. Lond. B. 1979

[4] Mascanzoni, D, Wallin, H "The harmonic radar: a new method of tracing insects in the field". Ecological Entomology, 1986

[5] Riley, JR, Smith, AD "Design considerations for an harmonic radar to investigate the flight of insects at low altitude". Comp. and El. in Agri., 2002

[6] Graham Brooker, "Introduction to sensors for ranging and imaging", 2009

[7] Data Sheet of Micro-space PC/104 plus CPU module

[8] Data Sheet FX 4400 strobe and PS4400 power supply

[9] Department of Agri. Fisheries and Forestry "Biology and behaviour of the Australian plague locust", 2008

[10] Data Sheet of camera

[11] Phil Green, Lindsay W. MacDonald, "Colour engg: achieving device independent colour" Vol. 385

[12] Nezamabadi, Mahdi "Technical Report Gain Measurement of the Sinarback 54 Digital Camera" 2005

[13] E Kurimo, L Lepistö, J Nikkanen, J Grén, I Kunttu and Jorma Laaksonen "The Effect of Motion Blur and Signal Noise on Image Quality in Low Light Imaging" Image Analysis16th Scandinavian Conference, SCIA, 2009

[14] Technical article on "Correction of CCD Image Imperfections", Diagnostics Instruments, Inc.

[15] Technical Note "CCD temperature variability and dark current correction", Mirametrics, Inc. USA

[16] Technical notes on "Dynamic Range" PCO imaging, Kelheim, Germany

[17] Data Sheet Sony ICX 204AK

[18] Wendel, A. "Feasibility of a retro reflector based locust tracker" undergraduate thesis, ACFR, University of Sydney, 2008

[19] Jeremy, R. "Technical Report on pixel size of XCD X710CR at different altitude", ACFR, University of Sydney

[20] Clissold, F.J., Sanson G.D., Read J. "Indigestibility of plant cell wall by the Australian plague locust, Chortoicetes terminifera" , Entomologia Experimentalis et Applicata, Vol 112, Issue 3, 2004

[21] Dept. of Agri and Food, Govt. of Western Australia, "Agricultural Memo", Vol 10, 2009